Engineering Tribology

J.A. WILLIAMS
Department of Engineering, University of Cambridge

OXFORD UNIVERSITY PRESS
OXFORD NEW YORK TOKYO
1994

$$p^* = \frac{1}{2}\left\{\gamma + \frac{\pi}{2} + \frac{\sin 2\gamma}{2} - \sec^2\gamma' \left[\frac{3}{4}\left(\gamma + \frac{\pi}{2}\right) + \frac{\sin 2\gamma}{2} + \frac{\sin 4\gamma}{8}\right]\right\} \tag{7.77}$$

where $\tan\gamma = \xi$ and, correspondingly, $\tan\gamma' = \xi'$.

Equation (7.77) gives the pressure distribution plotted as curve B in Fig. 7.12. The maximum value of p^* in this case is 0.127 and occurs when ξ' is equal to -0.475 (which point corresponds to values of $\gamma = 25.4°$ and $H = 1.23$). It follows from our definition of p^* in eqn (7.71) that the peak pressure p_{max} is given by

$$p_{max} = 2.15\bar{U}\eta\sqrt{\frac{R}{h_c^3}} \tag{7.78}$$

The load W/L carried by the discs can be found by straightforward integration. In non-dimensional terms,

$$W^* = \frac{Wh_c}{\eta R\bar{U}L} = 4.89. \tag{7.79}$$

When this is compared to the corresponding equation for the half-Sommerfeld boundary conditions (7.74) it can be seen that adopting the Reynolds boundary conditions has led to an *increase* in the estimated non-dimensionalised bearing load W^* from 4 to 4.89.

7.7 Plain journal bearings

Journal bearings are the most widely used form of machine component using hydrodynamic load support. A loaded, rotating shaft or *journal* is supported in a circular bush which has a slightly greater diameter. The geometry is shown in Fig. 7.13 (a). C is the centre of the journal and O the centre of the bush or bearing; c is the *clearance* or difference in radii between the journal and the bearing which is here shown very greatly exaggerated—in practice it is typically less than 1% of the bearing radius. Consider what happens if the shaft which carries a unidirectional load W starts to rotate with a small angular speed ω. The journal and the bearing surface are in contact at the point P and here a contact force R will be generated which is equal and opposite to the load W. This force R is often for convenience shown split into a pair of perpendicular components N and F, as shown in the figure: N is the normal contact force and F the frictional force which, since there must be sliding contact at P, is equal in magnitude to μN. The height of P above the lowest point in the bearing depends on the magnitude of the coefficient of friction μ at the contact point. To maintain the shaft in steady motion requires the application of a torque equal in magnitude to the couple formed by W and R.

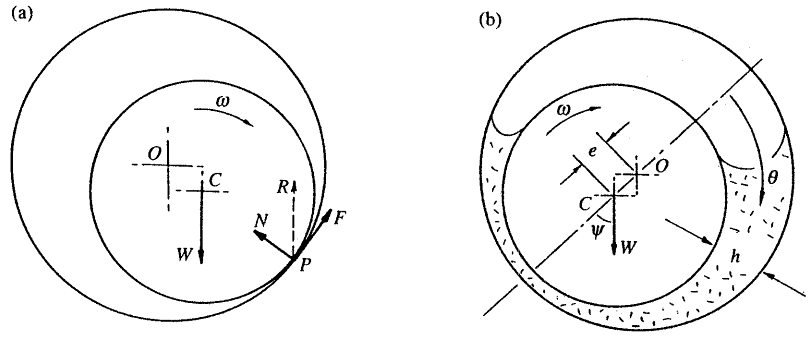

Fig. 7.13 Plain journal bearing; the journal rotates at speed ω, with (a) no lubrication present, or (b) hydrodynamic load support.

Now consider how the picture changes if both the bearing is supplied with a viscous lubricant and the speed of the journal is sufficient for hydrodynamic activity to be initiated. There is clearly a convergent wedge formed by the clearance gap on the upstream side of P: fluid is drawn into this gap pushing the solid surfaces apart. At some speed the point C will be vertically below the bearing centre O. However, this is rather a special circumstance; in general, the geometry will be as shown in Fig. 7.13 (b) with C to the left of O.

If the *eccentricity* or distance between the centres of the bearing and journal is designated by e then we can define an *eccentricity ratio* ε by the relation

$$\varepsilon = \frac{e}{c}, \tag{7.80}$$

and the minimum gap between the solid surfaces h_{min} is then given by

$$h_{min} = c - e = c(1 - \varepsilon). \tag{7.81}$$

To a satisfactory degree of accuracy for most purposes, the gap h will be related to the circumferential position θ by the equation

$$h = c(1 + \varepsilon\cos\theta) \tag{7.82}$$

where θ measures the angular position from the position of maximum film thickness. The line OC and the load vector will *not* be collinear and the angle ψ between them is known as the *attitude angle*.

7.7.1 *Narrow-bearing solution*

An important geometric parameter in the behaviour of journal bearings is the ratio of the bearing length to its diameter, L/D, in Fig. 7.14. In practice this ratio varies from about $\frac{1}{8}$ in the narrowest of journals to about 2. A 'square' bearing is one in which $L/D = 1$.

If the ratio of L/D is comparatively small, say less than $\frac{1}{4}$, then the short or narrow bearing analysis of Section 7.5 can be employed with acceptable accuracy. We have, from Section 7.5 for such a bearing, a parabolic pressure distribution, namely

$$p = \frac{12\eta}{h^3}\frac{dh}{dx}\bar{U}\left\{y^2 - \frac{L^2}{4}\right\} \tag{7.83}$$

provided that y, the axial position coordinate, is measured from the central section of the bearing. Combining this equation with (7.82) and noting that $\bar{U} = R\omega/2$, $x = R\theta$, and $dh/dx = -c\varepsilon/R\sin\theta$, we can write that the pressure distribution around the bearing is given by

$$p = \frac{3\pi\omega\varepsilon\sin\theta}{c^2(1+\varepsilon\cos\theta)^3}\left\{\frac{L^2}{4} - y^2\right\}. \tag{7.84}$$

Note that, because of the sine term, the distribution of pressure is antisymmetric about the line OC, that is, the full Sommerfeld conditions are implied, so that we are in effect supposing that the lubricant film is able to withstand large negative pressures.

An estimate of the load carried by this narrow journal bearing can be made by adopting the half-Sommerfeld boundary conditions, that is, by setting the film pressure equal to zero at values of θ between π and 2π, the range over which they would otherwise be negative. In this case, referring to Fig. 7.15,

$$W_z = \int_0^{\pi}\int_{-L/2}^{+L/2} pR\sin\theta\,dy\,d\theta \tag{7.85}$$

and

$$W_x = -\int_0^{\pi}\int_{-L/2}^{+L/2} pR\cos\theta\,dy\,d\theta. \tag{7.86}$$

Introducing the expression (7.84) for the pressure into these integrals leads to the expressions

$$W_z = \frac{\eta R\omega L^3\varepsilon\pi}{4c^2(1-\varepsilon^2)^{3/2}} \quad \text{and} \quad W_x = \frac{\eta R\omega L^3\varepsilon^2}{c^2(1-\varepsilon^2)^2}. \tag{7.87}$$

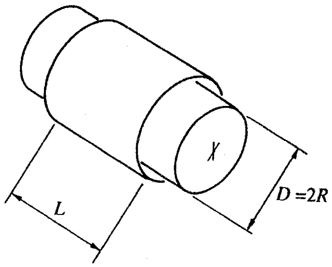

Fig. 7.14 Plain journal bearing length L and diameter D $(=2R)$; in a narrow bearing $L/D < 0.25$.

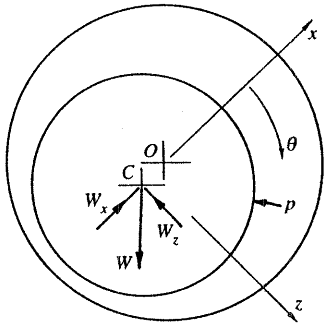

Fig. 7.15 Loads on a journal bearing. The applied load W must be carried by the sum of the component W_x and W_z.

The magnitude of the total load W on the journal is given by that of the resultant of these two components, that is,

$$W = \sqrt{W_x^2 + W_z^2}$$

so that, after a little algebra

$$W = \frac{\eta R \omega L^3}{4c^2} \frac{\pi\varepsilon}{(1-\varepsilon^2)^2} (1 + 0.62\varepsilon^2)^{1/2}. \qquad (7.88)$$

Defining a non-dimensional load W^*, in this case, by the expression

$$W^* = \frac{W/L}{\eta R \omega} \left\{\frac{c}{R}\right\}^2 \qquad (7.89)$$

and using the fact that the shaft diameter $D = 2R$, eqn (7.88) becomes

$$W^* = \left\{\frac{L}{D}\right\}^2 \frac{\pi\varepsilon}{(1-\varepsilon^2)^2} (1 + 0.62\varepsilon^2)^{1/2}. \qquad (7.90)$$

Although we could express results in the analyses of journal bearings in terms of the non-dimensional number W^*, the more usual non-dimensional group is known as the *Sommerfeld number S*. In what follows we shall take S to be defined by

$$S = \eta\omega \frac{LD}{W} \left\{\frac{R}{c}\right\}^2 \qquad (7.91)$$

so that

$$S = \frac{2}{W^*}. \qquad (7.92)$$

In terms of the entraining velocity, the Sommerfeld number S can be written as

$$S = \frac{4\eta L\bar{U}}{W} \left\{\frac{R}{c}\right\}^2. \qquad (7.93)$$

Equation (7.90) therefore becomes

$$\frac{1}{S} = \left\{\frac{L}{D}\right\}^2 \frac{\pi\varepsilon}{2(1-\varepsilon^2)^2} (1 + 0.62\varepsilon^2)^{1/2}. \qquad (7.94)$$

Other definitions of the Sommerfeld number are possible and are sometimes used. Consequently, care must be taken to make certain of the form of this group when referring to design guides, manufacturers' data, and so on. In eqn (7.91) ω is measured in radians per second; another possible non-dimensional group S' is defined by the identity

$$\frac{1}{S'} = \frac{1}{\eta \mathfrak{N}} \frac{W}{LD} \left\{\frac{c}{R}\right\}^2 \qquad (7.95)$$

wherec $\mathfrak{N}$ is the rotational speed in revolutions per second; this definition is often found in American texts. It thus follows that

$$S' = 2\pi S. \qquad (7.96)$$

The *attitude angle* ψ of the bearing, that is, the angle between the load vector and the line joining the centres of the bearing and the journal, can be evaluated from the relation

$$\tan\psi = -\frac{W_z}{W_x} = \frac{\pi(1-\varepsilon^2)^{1/2}}{4\varepsilon}. \qquad (7.97)$$

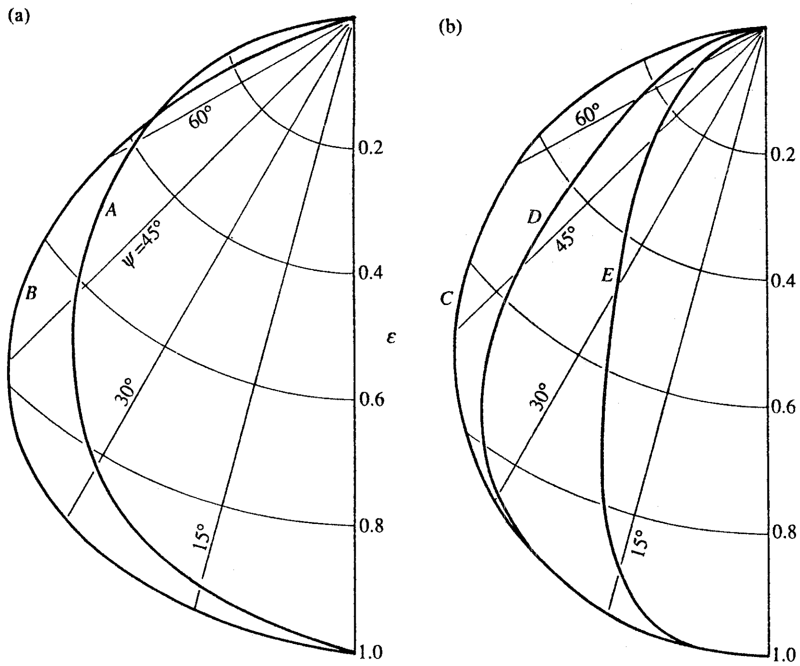

Fig. 7.16 Attitude angles, as functions of eccentricity ratio ε, for: (a) full 360° journal bearings A: the infinitely narrow bearing, B: the infinitely long bearing; and (b) journal bearings with $L/D = 1$ and included angles of C: 360°, D: 180°, and E: 60° (data from Raimondi and Boyd (1958) and Pinkus (1958)).

Figure 7.16(a), curve A, shows this relationship graphically as a polar plot. For *narrow* full bearings this curve is close to a semicircle in shape.

Figure 7.16(a), curve B, shows a corresponding plot for the infinitely long bearing, while Figure 7.16(b) illustrates the effect of changing the included angle of the journal for a square bearing ($L/D = 1$). Bearings with a reduced included angle, that is, partial bearings which do not completely enclose the shaft, can have some practical advantages; see Section 7.7.3.

An important practical matter in the design of the lubricant system is the volumetric flow rate of fluid through the bearing. Adopting the half-Sommerfeld boundary conditions, that is, supposing that pressure is zero at values of the angle θ between π and 2π, the flow of lubricant per unit length at entry Q_{in}, and exit Q_{out} of the convergent section are respectively

$$Q_{in} = \tfrac{1}{2}R\omega c(1+\varepsilon)L \quad \text{and} \quad Q_{out} = \tfrac{1}{2}R\omega c(1-\varepsilon)L. \qquad (7.98)$$

The difference between these two flows must leak from the ends of the bearing and so represents the flow which must be supplied to prevent the bearing becoming starved of lubricant. Expressed non-dimensionally as Q^*, the proportion of the volume flow rate supplied to the bearing, this loss is given by

$$Q^* = \frac{Q_{in} - Q_{out}}{Q_{in}} = \frac{2\varepsilon}{1+\varepsilon}. \qquad (7.99)$$

Figure 7.17 illustrates this relationship for the narrow bearing. Also plotted on the same axes are the relative make-up flows for two other plain journal bearings with length-to-diameter ratios of 1 and $\frac{1}{2}$.

7.7.2 *Long-bearing solution*

Pressure distribution and loads carried

A journal bearing whose length is more than about four times its diameter can reasonably be considered to be infinitely long; in this case there can be little or negligible axial lubricant flow. Conditions are governed by the one-dimensional form of Reynolds' equation given in eqn (7.9):

$$\frac{dp}{dx} = 12\eta\bar{U}\frac{h-\bar{h}}{h^3}, \qquad (7.9\ \text{bis})$$

where, as in the previous example, x is measured around the bearing circumference. To convert this equation to a more convenient form in cylindrical polar coordinates we can again replace x by $R\theta$ and $\bar{U}$ by $R\omega/2$. Also introducing eqn (7.82), which relates the gap h to the angular position θ, Reynolds' equation can be written in a normalized form as

$$\frac{dp^*}{d\theta} = \frac{c^2}{6R^2\eta\omega}\frac{dp}{d\theta} = \frac{1}{(1+\varepsilon\cos\theta)^2} - \frac{1+\varepsilon\cos\bar{\theta})}{(1+\varepsilon\cos\theta)^3}, \qquad (7.100)$$

where $\bar{\theta}$ identifies the position of the maximum pressure and p^* is a non-dimensional pressure defined by

$$p^* = \frac{c^2}{6R^2\eta\omega}p. \qquad (7.101)$$

Equation (7.100) can be solved explicitly in a number of ways. For example, making use of the *Sommerfeld substitution*,

$$\cos\gamma = \frac{\varepsilon + \cos\theta}{1+\cos\theta},$$

and using the boundary conditions that p^* falls to zero when θ takes the values 0 and 2π leads to the equation

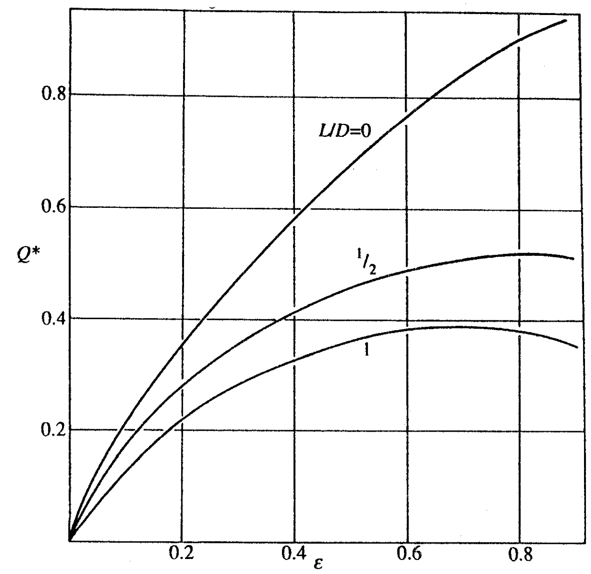

Fig. 7.17 Lubricant normalized make-up flows Q^* for full journal bearings of various L/D ratios plotted as functions of the bearing eccentricity ratio.

$$p^* = \frac{\varepsilon \sin\theta (2 + \varepsilon\cos\theta)^2}{(2+\varepsilon^2)(1+\varepsilon\cos\theta)^2}. \qquad (7.102)$$

The load on this infinitely long bearing can be evaluated in much the same way as that on the infinitely short bearing. Adopting the full Sommerfeld conditions and so allowing the possibility of negative pressures within the fluid, the expressions for the components of the load in the Ox- and Oz-directions of Fig. 7.15 become, respectively,

$$W_x = 0 \quad \text{and} \quad W_z = \frac{12\eta R^3 \omega L}{c^2} \frac{\pi\varepsilon}{(1-\varepsilon^2)^{1/2}(2+\varepsilon^2)}. \qquad (7.103)$$

Thus it follows from the definition of the Sommerfeld number, S, that

$$\frac{1}{S} = \frac{6\pi\varepsilon}{(1-\varepsilon^2)^{1/2}(2+\varepsilon^2)}. \qquad (7.104)$$

Additionally, we can note that since W_x is always zero, the attitude angle ψ must always be 90°, in other words, that the angle between the line of centres of the journal and the bearing is normal to the load line. The prediction that the locus of the shaft centre is a line perpendicular to the direction of the applied load seems at first sight unlikely, but is a natural consequence of the adoption of the *full* Sommerfeld conditions. For this to be a realistic picture, the fluid forming the film must not cavitate, which means that the negative pressures over the region $\pi < \theta < 2\pi$ must be small, well below one atmosphere. In fact, under these circumstances there is good experimental evidence that the shaft locus is close to that predicted.

The preceding analytic solutions can easily be adapted, by changing the limits of integration, into the half-Sommerfeld conditions. These discount the lobe of negative pressure but suffer the disadvantage of introducing a significant discontinuity in flow at the position $\theta = \pi$ or 180°. More satisfactory is the adoption of the Reynolds' conditions, that is, to seek a pressure distribution which is consistent with an exit point at which both p and its derivative $dp/d\theta$ are zero. In this case the film extends beyond the point of minimum clearance (at which $\theta = 180°$) by the angle θ'. Table 7.3 gives some values for this angle as well as other performance parameters of such an infinitely long bearing.

In practice the bearing designer must choose an acceptable combination of the values of the Sommerfeld number (which is a measure of the severity of the bearing duty) and the eccentricity ratio which will leave the minimum gap sufficiently large both to make solid contact between the asperities on the surfaces of the journal and the bearing unlikely, and reduce damage arising from the entrainment of abrasive dirt or contaminant in the oil. A typical, if rather conservative, design value of ε might be about 0.6, and Fig. 7.18 illustrates the circumferential pressure distribution (plotted non-dimensionally as p^*) according to both Sommerfeld (curve A) and Reynolds (curve B) boundary conditions for an eccentricity ratio of this magnitude. Also shown, as curve C, for comparison is the Sommerfeld curve for a value of $\varepsilon = 0.4$.

As well as the effect of the value of the Sommerfeld number on the eccentricity ratio (and hence the minimum film thickness) we may also be interested in the location of the point where this occurs, relative to the load

Table 7.3 The behaviour of the infinitely long journal bearing with Reynolds boundary conditions; variables are defined in the text.

S	2.99	1.52	0.78	0.53	0.40	0.31	0.24	0.19	0.13	0.07	0.04
ε	0.05	0.1	0.2	0.3	0.4	0.5	0.6	0.7	0.8	0.9	0.95
W^*	0.67	1.32	2.57	3.80	5.06	6.46	8.17	10.6	15.1	27.7	52.3
ψ (°)	70.0	69.0	66.9	64.5	61.6	58.3	54.2	49.1	42.2	31.7	23.2
θ' (°)	73.3	69.2	61.3	53.8	46.6	39.7	33.1	26.6	20.2	13.2	9.0
M^*	6.24	6.23	6.35	6.64	7.11	7.78	8.75	10.2	12.7	18.1	25.8

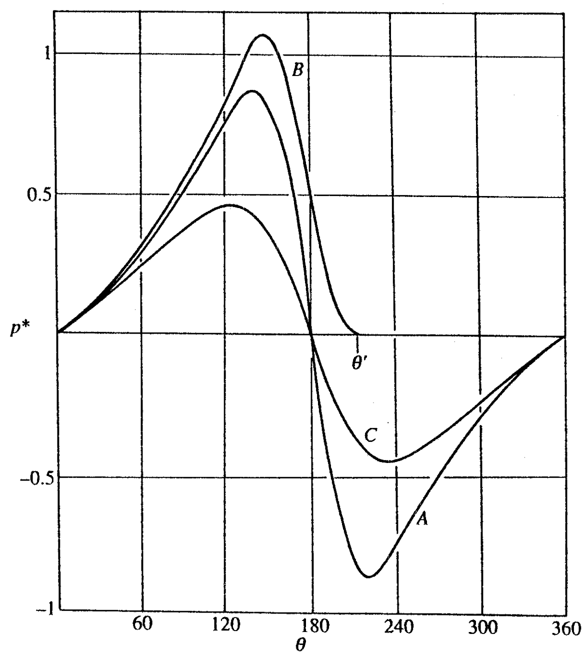

Fig. 7.18 Circumferential non-dimensional pressure distribution p^* around a 'long' journal bearing; curves A and C are for Sommerfeld boundary conditions with $\varepsilon = 0.6$ and $\varepsilon = 0.4$ respectively, and curve B is for Reynolds boundary conditions with $\varepsilon = 0.6$.

line. This information is provided by the attitude angle ψ, and the variation in this with ε for a long full (i.e. 360°) bearing is also given in Table 7.3 and displayed in Fig. 7.16 as curve B; curve A is the corresponding information for an infinitely short bearing.

Observation in the field suggests that some bearings operate satisfactorily for periods at which their eccentricity ratios are very high, perhaps in excess of 0.9, and thus with their surfaces separated by very thin lubricant films. The thickness of the predicted lubricant film under these conditions may well be less than the asperity size on the journal and bearing. Were the solid surfaces to be absolutely rigid and undeformable this would imply significant areas of true contact between them and so we should expect considerable consequential damage and wear, which is often not in fact observed. The explanation for the successful operation of such contacts lies principally in the local elastic flattening of surface roughnesses that takes place within the confines of the contact zone; these *elasto-hydrodynamic* effects are considered more fully in the following chapter.

7.7.3 *Practical considerations*

Slenderness ratio

The influence of the bearing Sommerfeld number on the eccentricity ratio for full journal bearings of various values of L/D or *slenderness ratio* is summarized in Fig. 7.19. Increasing the load on the bearing reduces the numerical value of the Sommerfeld number S and so the operating point must move from right to left. Thus for a bearing of a particular value of L/D the eccentricity ratio increases. Once the slenderness ratio has fallen to about $\frac{1}{4}$ the situation is effectively dominated by axial lubricant flow and so the short-bearing analysis of Section 7.7.1 can be applied; the short-bearing solution, eqn (7.94), is shown dotted in Fig. 7.19. Also on this diagram are displayed the results from the application of the half-Sommerfeld and Reynolds boundary conditions to the infinitely long bearing.

From a practical point of view there are limits on both the maximum and minimum values of the L/D ratios that can be sensibly used. If this ratio is too low, that is much less than about $\frac{1}{4}$, then the volumetric flow rate demanded by the bearing becomes excessively large for the load that can be supported. On the other hand, if L/D is much more than about 2 there can be difficulties in satisfactorily aligning the journal and bearing. Even if these can be set up with the shaft unloaded, subsequent elastic flexing under the action of the applied and dynamic loads can lead to unacceptably thin lubricant films at the edges of the bearings. The recommended design range is indicated by the area with the dashed perimeter.

Friction in journal bearings

The presence of a film of viscous lubricant between the journal and the bearing means that a torque must be continuously supplied to maintain rotation of the bearing elements. If the journal and the bearing were concentric then the velocity gradient across the fluid film would be equal to $R\omega/c$ and thus the frictional torque M/L per unit length would simply be given by

$$\frac{M}{L} = \frac{2\pi\eta\omega R^3}{c}. \qquad (7.105)$$

This is known as the *Petrov equation*, and can be used to provide a quick estimate of the frictional effects in a real design, even when the actual operating value of ε is unknown. In practice, we know that the journal and the bearing will not be concentric, but will operate at some characteristic value of the eccentricity ratio ε. Nevertheless, friction effects can be accounted for: taking the case of an infinitely long bearing operating with a full fluid film between the solid surfaces, we can evaluate the total drag force F experienced by the shaft. F represents the integration around the circumference of the viscous shear force and is given by the equation

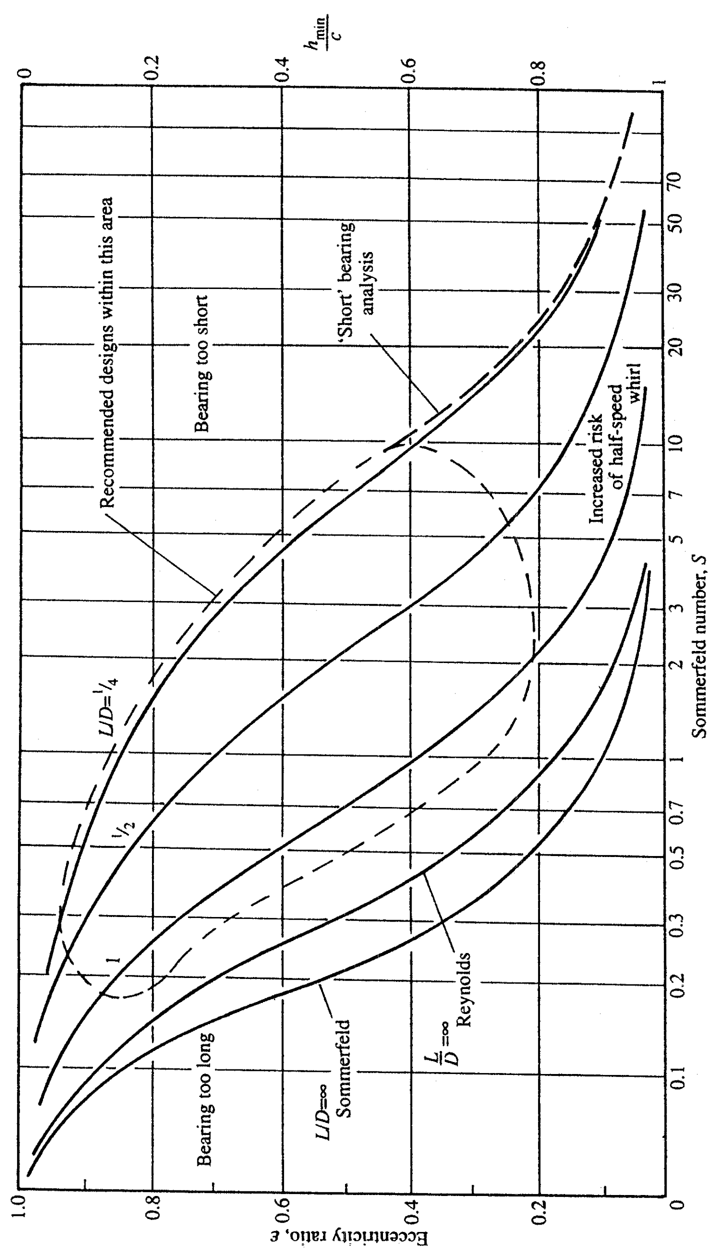

Fig. 7.19 Eccentricity ratio ε versus Sommerfeld number S for 360° journal bearings of various L/D ratios (data from Raimondi and Boyd (1958)).

$$F = \frac{4\pi\eta\omega R^2 L}{c} \frac{1 + 2\varepsilon^2}{(2 + \varepsilon^2)(1 - \varepsilon^2)^{3/2}}. \tag{7.106}$$

We can relate the value of the eccentricity ratio ε to the Sommerfeld number S and this means that the drag force F can also be expressed in terms of S. One way of displaying such a relationship in a non-dimensional form is to define a coefficient of friction μ for the bearing as F divided by the bearing load W. From eqns (7.103) and (7.106) it follows that for an infinitely long bearing operating with the full Sommerfeld conditions

$$\mu \left\{\frac{R}{c}\right\} = \frac{1 + 2\varepsilon^2}{3\varepsilon}. \tag{7.107}$$

This equation indicates that friction will be a minimum when the eccentricity ratio ε has the numerical value $1/\sqrt{2} = 0.71$. Although the prediction of a minimum frictional resitance is perhaps rather more a result of the idealizations made in the analysis than a true representation of realtity, this value of ε is not unrepresentative of many practical steadily loaded journal bearings. Figure 7.20 shows some curves of $\mu(R/c)$ versus S for full journal

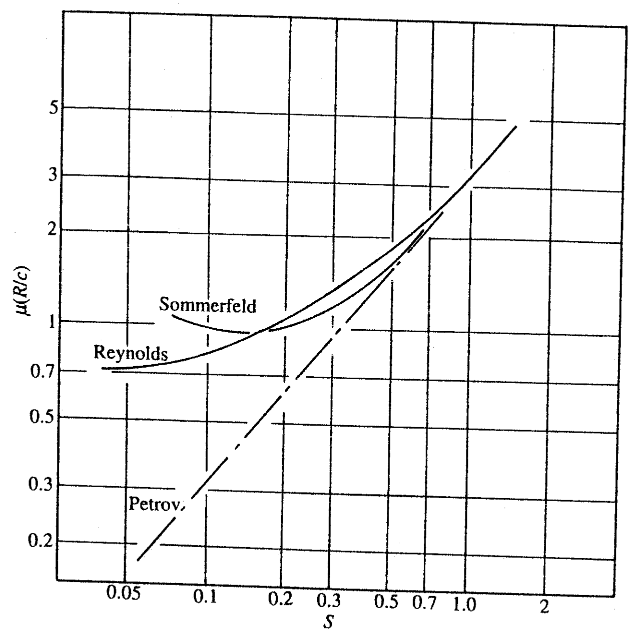

Fig. 7.20 Bearing friction plotted as $\mu(R/c)$ versus Sommerfeld number S for full journal bearings with $L/D \gg 1$ (data from Raimondi and Boyd (1958)).

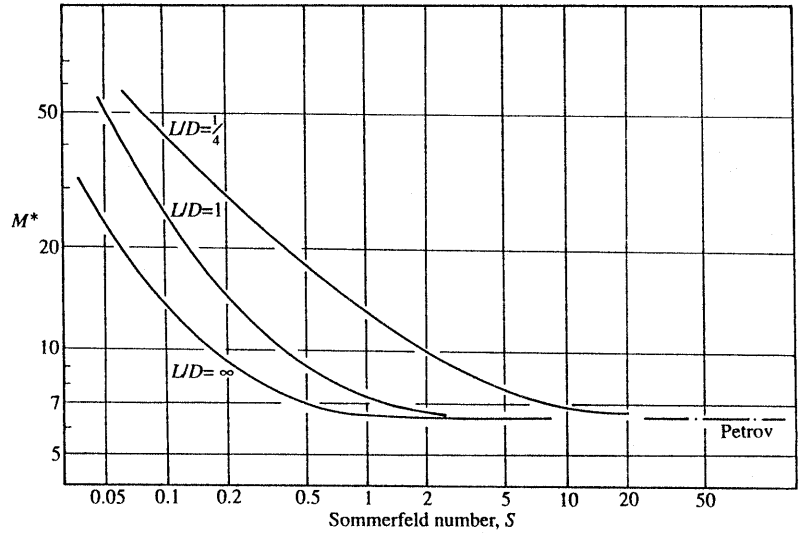

Fig. 7.21 Non-dimensional friction torque M^* versus Sommerfeld number S full journal bearings (data from Raimondi and Boyd (1958)).

bearings with both Sommerfeld and Reynolds boundary conditions. Also shown is the line corresponding to the Petrov equation (7.105).

The frictional torque M on the bearing is simply given by $F \times R$; this can be suitably non-dimensionalized to M^*, where

$$M^* = \frac{Mc}{\eta \omega R^3 L}. \tag{7.108}$$

Figure 7.21 provides plots of M^* versus S for bearings with three slenderness ratios. At higher values of S the curves become asymptotic to the Petrov solution.

It is worth noting that a further consequence of the lack of concentricity between the journal and the bearing is the fact that the frictional torques experienced by each of these components are not the same; that on the journal exceeds that on the bearing by an amount ΔM, where

$$\frac{\Delta M}{M} = \frac{2\varepsilon \sin\psi}{SM^*}. \tag{7.109}$$

This effect may not be negligible, for example, if $\varepsilon = 0.6$, $S = 0.4$, and $M^* = 12$ then $\Delta M/M$ might be as great as 25 per cent.

Partial journals

It is clear from an examination of the pressure profile of Fig. 7.18 that only a portion of the circumference of the bearing actually carries the applied load; this 'effective' arc extends to rather more than 180°. Viscous losses in the film, on the other hand, are generated all the way around the circumference. In those cases in which the load line is in a fixed and known direction it may be sensible, from an energy-saving point of view, to use a bearing with a restricted arc of contact, of perhaps 180° or sometimes even less. In this way viscous losses may be reduced by a significant factor compared to the full bearing. Figure 7.22 illustrates the relationship between the angle of the bearing arc β and the Sommerfeld number S for bearings with three different slenderness ratios, all operating at an eccentricity ratio of 0.6. In these cases it has been assumed that the load vector bisects the angle β. Figure 7.23 illustrates the effect that the extent of the bearing arc has on the relationship between the frictional torque M^* and the Sommerfeld number for three cases each with a ratio of $L/D = 1$. Once again the curves are asymptotic to the Petrov solutions at higher values of S. The effects of these restricted ares of contact on the value of the attitude angle is shown in Fig. 7.16(b).

Lubricant supply

Lubricant is usually fed to a plain journal bearing through a pocket, groove, or hole located in the unloaded arc of the bearing shell, in the manner illustrated in Fig. 7.24. In oil lubrication, the supply pressure is typically between 70 and 350 kPa (10–50 psi) which is very much less than the hydrodynamic pressures generated over the loaded area of contact. Although the bearing does not depend directly on this pressure to carry the applied load it is essential that a continuous supply of lubricant is maintained if the bearing is not to suffer from oil starvation and possible collapse. In practice, full journals are invariably split into two halves, each subtending an angle of 180°, mechanically clamped together. It is usual to assume that the joint between them is oil-tight and so does not affect the operation of the bearing. The standard position for the oil feeds will be at 90° to this parting line as indicated in Fig. 7.24(a), although this can be modified if the load on the bearing is always unidirectional. If the bearing is reasonably long then the oil hole may supply an oil feed pocket extending some way axially along the bearing, as illustrated in Fig. 7.24(b). In cases where the load vector is variable in direction the oil feed pocket may extend around the bearing circumferentially, as shown in Fig. 7.24(c). Although this arrangement will prevent oil starvation, whatever the load direction, it is at the cost of splitting the bearing into two independent halves each with a slenderness ratio of half the original value.

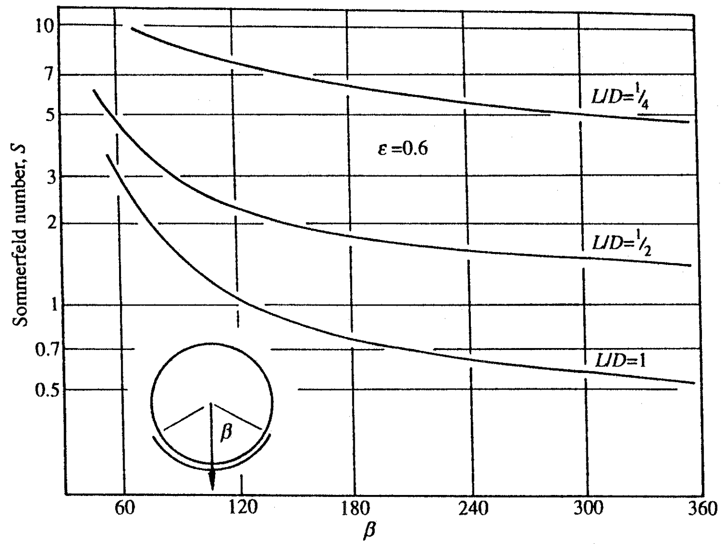

Fig. 7.22 Partial journal bearings: influence of the included angle β on the Sommerfeld number for L/D ratios of 1, $\frac{1}{2}$, and $\frac{1}{4}$. The load vector bisects the included angle (data from Raimondi and Boyd (1958)).

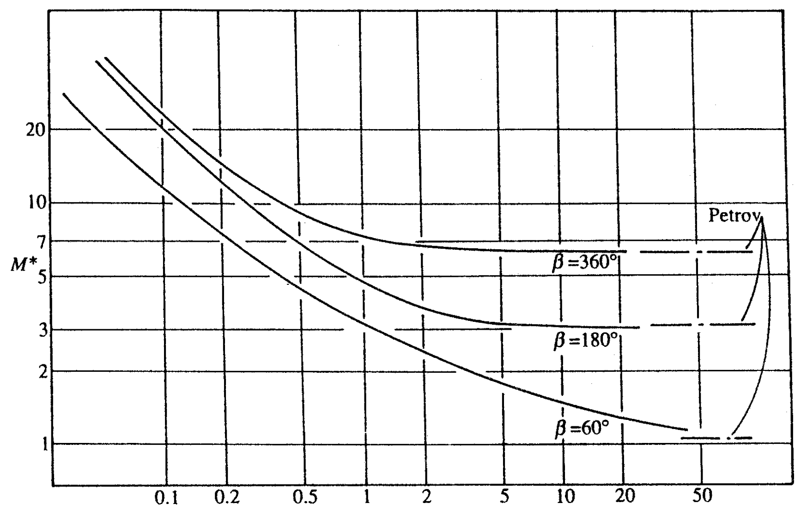

Fig. 7.23 Partial journal bearings: influence of the bearing arc angle on the relationship between M^* and S (data from Raimondi and Boyd (1958)).

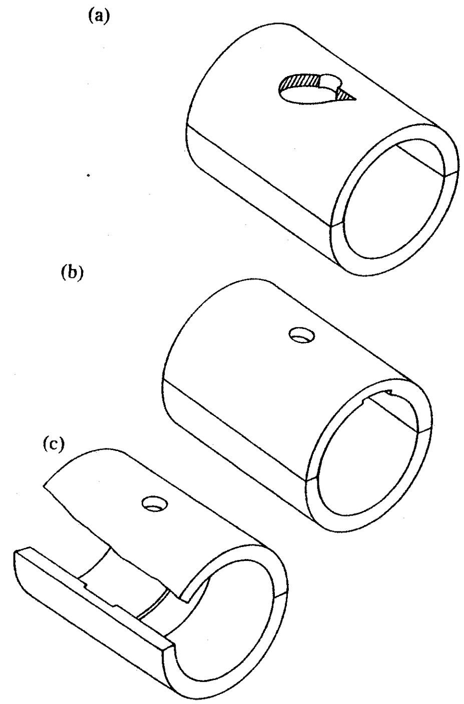

Fig. 7.24 Oil supply arrangements in plain journal bearings: (a) single oil hole; (b) axial oil feed pocket; and (c) circumferential oil feed pocket.

7.8 Thermal effects in lubricated journal bearings

The shaft size, rate of rotation, and radial applied load of a journal bearing are usually design parameters outside the decision of the bearing designer who will be asked to suggest a satisfactory tribological design involving the specification of bearing length and clearance, and the materials, oil viscosity (or grade), and flow rate. We have seen that an important decision is the choice of the steady eccentricity ratio ε, since the minimum film thickness and so the tolerance that the bearing is likely to display to contamination or surface irregularities or degradation depends on the combination of its value and that of the clearance c. Setting the bearing clearance too high will result in excessive oil flow requirements, and so unrealistically expensive supply pumps and feed arrangements; on the other hand, setting the clearance too low will bring about premature bearing failure through solid-to-solid or rubbing contact. In service, frictional shearing of the oil film will increase the local temperature of the oil and so reduce its viscosity; some of this thermal energy is carried away by convection as the lubricant passes through the bearing, and some lost by conduction through the bearing and its housing and adjacent components.

For the case of a slider pad bearing (Fig. 7.1) Cameron and Ettles (1981) have suggested the following simple argument to determine, very approximately, the relative losses by conduction and convection. Suppose that the lower moving surface is maintained at ambient temperature while that of the upper pad increases linearly from ambient at entry (where $x = 0$) to a maximum $\Delta\Theta$ above ambient at $x = B$. At a point on the surface of the pad with coordinate x, the temperature rise will be equal to $\Delta\Theta x/B$. If we also now take the temperature gradient *across* the oil film as linear, and use an average film thickness h, this gradient will be equal to $\Delta\Theta x/Bh$. The rate of local heat flow per unit area by conduction will thus be $K \times \Delta\Theta x/Bh$ where K is the thermal conductivity of the lubricant. This expression can be integrated to give the total heat flow per unit width of bearing, namely

$$\dot{H}_{cond} = \int_0^B \frac{\Delta\Theta x}{Bh}\,dx = \frac{\Delta\Theta}{h}\frac{KB}{2}. \tag{7.110}$$

Heat flow by convection $\dot{H}_{conv}$ is simply the product of the mass flow of oil, its specific heat, and average temperature rise $\Delta\Theta/2$. Thus

$$\dot{H}_{conv} = \frac{Uh\rho c}{2} \times \frac{\Delta\Theta}{2}. \tag{7.111}$$

We can thus write that the ratio of conducted to convected heat is equal to

$$\frac{\dot{H}_{cond}}{\dot{H}_{conv}} = \frac{K}{\rho c}\frac{2B}{Uh^2} \tag{7.112}$$

$\Delta\Theta$ can thus be estimated from eqns (7.111) and (7.112) since $\dot{H} = \dot{H}_{cond} + \dot{H}_{conv}$ will be equal to the total energy dissipation in the bearing; see eqn (7.43). The lubricant property group $K/\rho c$ is known as its diffusivity κ (see Chapter 3), and for mineral oils has a value of approximately $0.08 \times 10^{-6}\,m^2\,s^{-1}$. This form of simple argument can be extended to journal bearings when it suggests that the ratio of conducted to convected heat is now given by

$$\frac{\dot{H}_{cond}}{\dot{H}_{conv}} = \kappa \times \frac{4\pi}{\omega R^2}\left\{\frac{R}{c}\right\}^2. \tag{7.113}$$

As we should expect, convection becomes increasingly important at higher bearing speeds.

The full analytical treatment of this thermal balance problem, leading to

estimates of actual bearing and lubricant temperatures, is likely to be both difficult and time-consuming as it requires simultaneous solution of the lubrication equations together with the equations of heat flow both in the oil film and the metallic components. Below are suggested some much simplified but rapid procedures which can be used to obtain rough estimates of the likely temperature rises in real cases and can thus assist in the choice of design parameters and lubricant grades. In many cases, for the sake of compactness, the hope will be to specify a bearing with a length L less than its diameter D. If we choose to make $L/D = 0.5$, then as a first approximation we might adopt the short-bearing analysis of Section 7.7.1, in which we showed that

$$\frac{1}{S} = \left\{\frac{L}{D}\right\}^2 \frac{\pi\varepsilon}{2(1-\varepsilon)^2}(1 + 0.62\varepsilon^2)^{1/2} \tag{7.94 bis}$$

where S is the Sommerfeld number defined by eqn (7.91). A sensible working compromise for the value of ε is 0.7 and a 'standard' value for the radial clearance ratio c/R (i.e. $2c/D$) might well be 0.001, so it follows, by substituting this data, that

$$\eta = \frac{WD}{\omega L^3} \times 2 \times 10^{-7} \tag{7.114}$$

where η is the effective viscosity of the lubricant in the bearing gap.

Even though the centre of any journal is likely to be displaced relative to that of the bearing the power loss can be reasonably approximated by idealizing them as running concentrically, so that the frictional moment can be taken from the Petrov equation (7.105). The rate of dissipation of energy $\dot{H}$ in the bearing is then

$$\dot{H} = M \times \omega = \frac{2\pi R^3 L}{c}\eta\omega^2. \tag{7.115}$$

If we make the assumption that all this thermal energy is carried away by convection via the flow of oil through the bearing then, using eqns (7.98) and (7.99), we can write that

$$\dot{H} = \frac{2\varepsilon}{1+\varepsilon} \times \rho c \Delta\Theta \times (1+\varepsilon)\frac{R\omega Lc}{2}, \tag{7.116}$$

where ρ and c are the density and specific heat of the oil respectively, and $\Delta\Theta$ is the temperature rise. Setting ε to 0.7, and taking note that for mineral oils ρ is very close to $900\,kg\,m^{-3}$ and c is approximately $1.88\,kJ\,kg^{-1}\,K^{-1}$, we can say that

$$\Delta\Theta \approx \frac{2\pi}{\varepsilon}\left\{\frac{R}{c}\right\}^2 \frac{\omega\eta}{\rho c} \approx 5.30\,\omega\eta. \tag{7.117}$$

The problem is therefore to identify a value of η which is consistent with both eqns (7.114) and (7.117) and the physical characteristics of the oil, in particular the way in which its viscosity varies with temperature. This behaviour has been discussed for a range of practical mineral oils in Section 1.3.

For example, suppose the problem is to place a limit on the inlet temperature of SAE30 oil supplied to a journal bearing of radius $R = 0.025$ m and length $L = 0.025$ m with $c/R = 0.001$ carrying a load of 4500 N at 1000 rpm. Here $L/D = 0.5$, $\omega = 104.7$ rad s^{-1} and so from eqn (7.114)

$$\eta = \frac{4500 \times 0.05}{104.7 \times 0.025^3} \times 2 \times 10^{-7} = 0.0275 \text{ Pa s}$$

But, from eqn (7.117) the corresponding temperature increase $\Delta\Theta$ is given by

$$\Delta\Theta = 5.3 \times 104.7 \times 0.0275 = 15.3°\text{C}.$$

We can now refer to Fig. 1.10 to establish that SAE30 oil has a viscosity of 0.0275 Pa s at a temperature of approximately 65°C and hence the oil should enter the bearing at a temperature of (65 − 15)°C, that is at no more than 50°C.

The Engineering Sciences Data Unit publication 66023 (see Appendix 2) contains a much fuller iterative procedure for establishing the steady state running conditions of lubricated journals. The aim must be to ensure that the minimum film thickness will be adequate to prevent mechanical surface damage without the maximum bearing and oil temperature being so large as to lead to premature thermal degradation of either. The general form of these limitations can be displayed on axes representing journal speed and radial load; see Fig. 7.25. At low speeds and high loads, and so small film

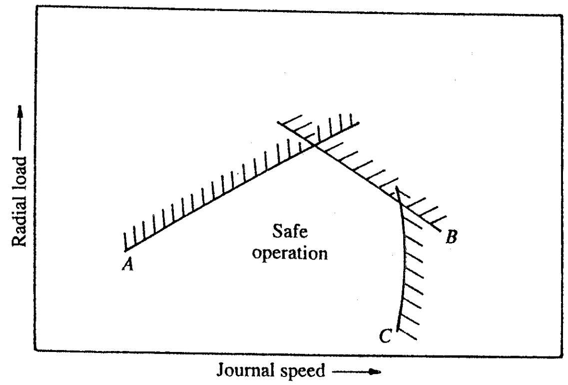

Fig. 7.25 Limits for the satisfactory operation of hydrodynamically lubricated journal bearings: (*A*) scuffing; (*B*) wiping; and (*C*) chemical degradation.

thicknesses, there is the danger of true metallic contact with its associated scuffing and scoring; this limitation gives line A on this map of bearing operation. At high speeds and high loads if metallic contact occurs then the high sliding speed may lead to the generation of surface temperature sufficient to perhaps soften or even locally melt the bearing alloy leading to smearing or wiping of the surface; this limitation is shown as line B. Finally at even higher speeds but low loads the very high rates of shear in the oil film may lead to lubricant temperatures becoming so great that there is a danger of chemical degradation, principally excessive oxidation; this effect gives the limit illustrated by line C.

Figure 7.26 summarizes the procedures set out by Martin and Garner (1974) and which enables the dimension of the minimum film thickness to be estimated in an oil-lubricated journal bearing. Basically, three 'grids' are used to define the problem and by linking these along the appropriate guide lines a point in the fourth 'solution' grid is obtained. (The lower case letters a to m allow the transfer of data between parts (a) and (b) of the figure.) In the previous design example the inputs to the design are the clearance ratio c/R, the length-to-diameter ratio L/D, the speed, oil grade, and the specific bearing load, W/LD, and these have the numerical values 0.001, 0.5, 105 s^{-1}, SAE 30, and 3.6 MPa respectively. Using the arrows as indicated in Fig. 7.26 produces an estimated value of ε of approximately 0.75 so that $h_{min} = (1 - 0.75) \times 0.001 \times R = 6.3$ microns. Figure 7.26 is based on the design of a plain journal bearing in which the bearing gap is supplied by two axial oil grooves with lubricant at a pressure of 100 kPa (i.e. about 15 psi).

The maximum oil temperature Θ_{max} occurs within the lubricant film at a position which roughly coincides with that of the minimum film thickness. Figure 7.27 can be used to estimate its value. An example of the use of the chart is provided in the figure in which Θ_{eff} represents the 'effective' temperature of the oil, which is assumed to enter the bearing at 50°C; conditions are as for the example in Fig. 7.26.

7.9 Dynamic effects in hydrodynamic bearings

7.9.1 *Squeeze films effects*

Journal bearings

In our analyses of journal bearings we have made the assumption that the load is steady with time. Although many bearings do operate under conditions that approximate to this, there are many devices within which bearings are subject to loads which are constantly changing. As a result of these fluctuations, the lubricant is alternately squeezed out and drawn into the bearing gap; this imposed motion, combined with the viscosity of the lubricant, results in a contribution to the load-carrying capacity which is